We are IntechOpen,
the world's leading publisher of
Open Access books
Built by scientists, for scientists

6,900
Open access books available

186,000
International authors and editors

200M
Downloads

Our authors are among the

154
Countries delivered to

TOP 1%
most cited scientists

12.2%
Contributors from top 500 universities

CLARIVATE ANALYTICS

BOOK
CITATION
INDEX

INDEXED

WEB OF SCIENCE™

Selection of our books indexed in the Book Citation Index
in Web of Science™ Core Collection (BKCI)

Interested in publishing with us?
Contact book.department@intechopen.com

Clear-Water Scour at Labyrinth Side Weir Intersection Along the Bend

M. Emin Emiroglu
Firat University
Turkey

1. Introduction

Weirs are among the oldest and simplest hydraulic structures, and have been used for centuries by hydraulic and environmental engineers for flow measurement, flow diversion, regulation of flow depth, flood passage, and other means. Although the definition of many different kinds of weirs is very simple and similar, the application and hydraulic behavior of each is quite different (Borghei *et al.*, 1999). Weirs are normally placed perpendicular to the direction of flow of the main channel. The most significant parameters in determining the capacity of a weir are its height relative to the upstream depth, the crest shape, and the crest length. Here, capacity refers to the flow rate or discharge for a given depth of flow over the crest of the weir. Of these parameters, the crest length has the greatest influence on the discharge capacity. The crest length can be increased further and can still keep the downstream dimension small by folding the weir into several sections. One implementation of this idea is the duckbill spillway (Falvey, 2003). A Labyrinth weir is an overflow weir folded in plan view to provide a longer total effective length for a given overall weir width. A Labyrinth weir has advantages compared to the straight overflow weir and the standard ogee crest. The total length of the labyrinth weir is typically three to five times the weir width. Its capacity varies with head and is typically about twice that of a standard weir or overflow crest of the same width (Tullis *et al.*, 1995). Labyrinth weirs have long been used as the spillway of a dam reservoir. Emiroglu *et al.* (2010) used the labyrinth weirs as a side weir structure. If the crest is placed parallel with the channel centerline, it is called a side weir. A side weir is an overflow weir framed in the side of a channel, which allows lateral overflow when the surface of the liquid in the channel rises above the weir crest. Side weirs, also known as a lateral weir, are control structures, widely used in canal systems and for storm water overflow from urban drainage systems. Like normal weirs, side weirs may be sharp, broad or rounded-crested. In addition, flow in the main channel along a side weir may be subcritical or supercritical.

The flow over a side weir falls within the category of spatially varied flow. The existing studies of side weir flow deal mainly with the application of the energy principle. The energy principle assumes that the longitudinal component of velocity vector of spill flow at any section is equal to the average velocity of flow in the channel. Therefore the total energy per unit mass of water remaining in the channel is unaffected by the spill flow occurring and, apart from frictional losses, the total energy of the flow in the main channel remains constant. The concept of constant specific energy (De Marchi, 1934) is often adopted when

studying the flow characteristics of these weirs. The discharge over the side weir per unit length, *q*, is assumed as:

$$q = -\frac{dQ}{ds} = C_d\sqrt{2g}\,[h - p]^{3/2} \tag{1}$$

where Q is the discharge in the main channel, s is the distance from the beginning of the side weir, dQ/ds (or q) is the spill discharge per unit length of the side opening, g is the acceleration due to gravity, p is the crest height of the side weir, h is the depth of flow at the section s (at $s=0$: $h=h_1$ and $Q=Q_1$), (h-p) is the pressure head on the weir, and C_d is the discharge coefficient (De Marchi coefficient) of the side weir (see Fig. 1). In which C_d is dimensionless, g is m/s² and, h and p are in meters. Thus, the discharge within the main channel at the downstream end of the side weir can be written as:

$$Q_2 = Q_1 - Q_w \tag{2}$$

where Q_2 is the discharge within the main channel at the downstream end of the side weir and Q_1 is the total discharge within the main channel at the upstream end of the side weir.
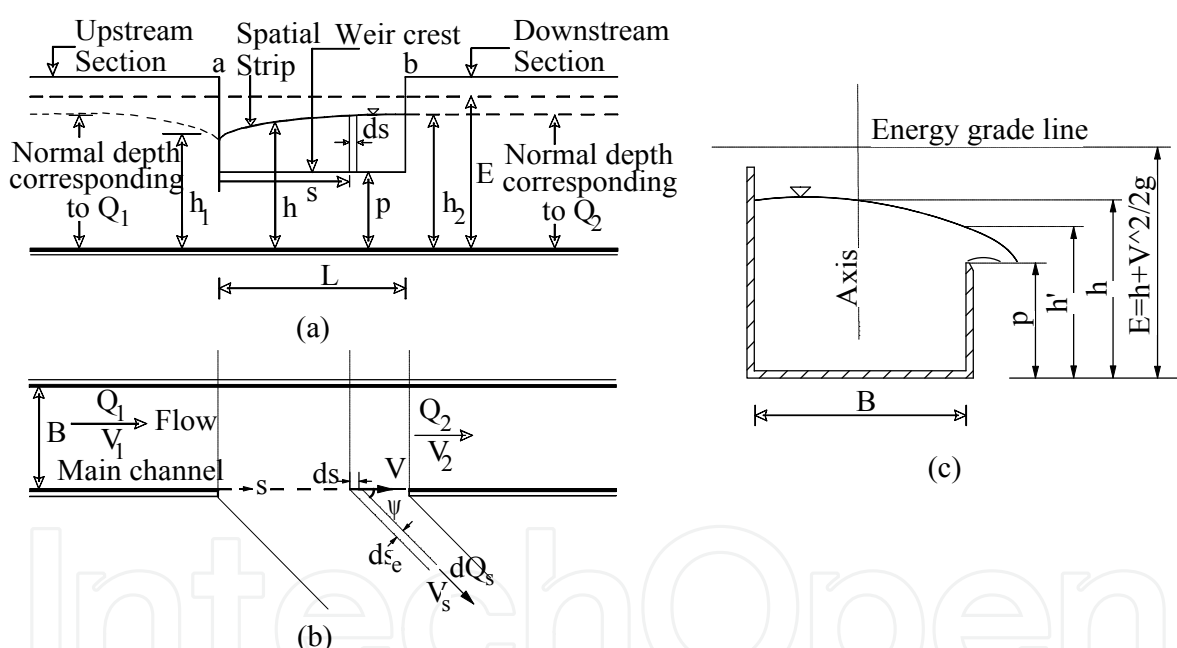
Fig. 1. Definition sketch of subcritical flow over a side weir: (a) Longitudinal section of the side weir, (b) Plan view of the side weir, (c) Front view of the side weir.

2. Experimental set-up and experiments

Labyrinth side weir experiments were conducted at the Hydraulic Laboratory of Firat University, Elazig, Turkey (Emiroglu *et al.*, 2007). A schematic representation of the experimental set-up is shown in Fig. 2. The experimental set-up consisted of a main channel and a discharge collection channel. The main channel was 12 m long and the bed had a rectangular cross-section. The main channel was 0.5 m wide, 0.5 m deep, with a 0.001 bed slope. The channel was constructed from a smooth, horizontal, well-painted steel bed with

vertical glass sidewalls. A sluice gate was fitted at the end of the main channel in order to control the depth of flow. The collection channel was 0.5 m wide and 0.7 m deep, and was situated parallel to the main channel. The width of the collection channel across the side weir was 1.3 m and constructed in a circular shape, to provide free overflow conditions. A rectangular weir was placed at the end of the collection channel, in order to measure the discharge of the side weir. A Mitutoyo digital point gauge with ±0.01 mm sensitivity was fixed at a location 0.4 m from the weir. Trapezoidal labyrinth side weirs were produced from steel plates, which had sharp edges and were fully aerated. These were installed flush with the main channel wall.

Experiments were conducted at subcritical flow, stable flow conditions and free overflow conditions. Surface tension σ is an important parameter for small nape heights. Novak & Cabelka (1981) reported that minimum nape height over side weirs should not be less than 30 mm because of the surface tension over the weir crest. As mentioned above, the minimum nape height over the side weir is taken as 30 mm. Therefore, the influence of surface tension can be ignored.
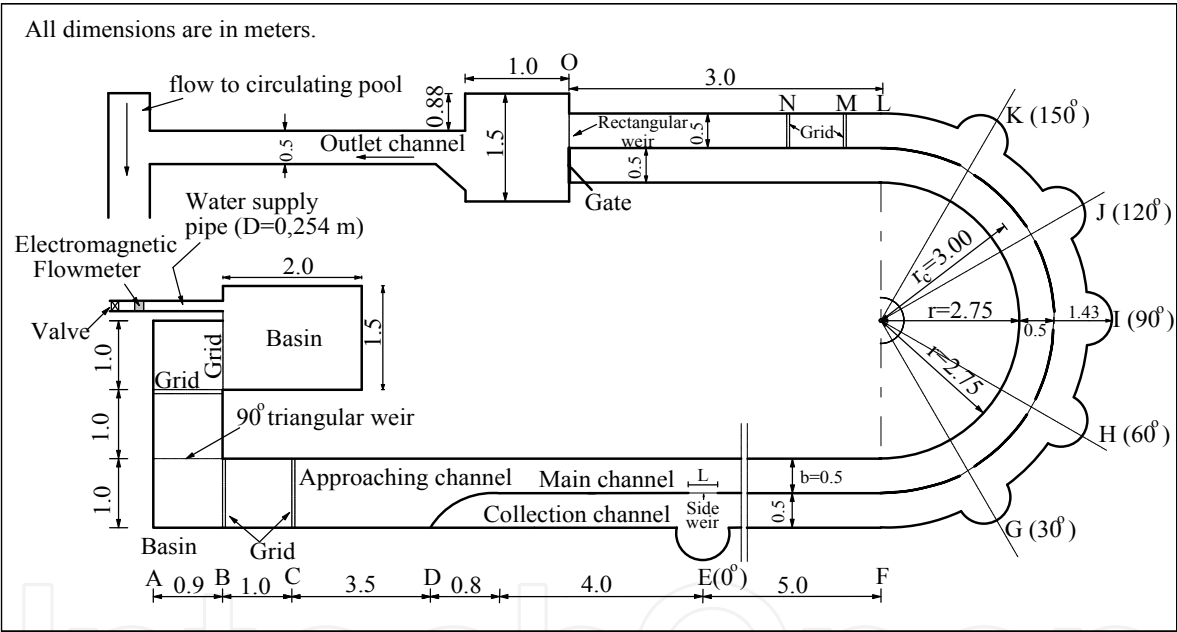

Fig. 2. Experimental arrangement.

3. Discharge coefficient for labyrinth side weirs

3.1 Triangular labyrinth side weir

Figure 3 shows schematic and plan view of a triangular labyrinth side weir with one cycle. Emiroglu *et al*. (2010) studied the discharge coefficient of sharp-crested triangular labyrinth side weirs on a straight channel. They obtained the following results regarding the labyrinth side weir discharge coefficient: (1) Discharge coefficient of the labyrinth side weir is 1.5 to 4.5 times higher than that of the rectangular side weir. (2) The discharge coefficient C_d increases when L/B ratio increases. A decrease in the labyrinth weir included angle θ causes a considerable increase in C_d, due to increasing the overflow length. A labyrinth side weir with θ=45° was shown to have the greatest C_d values of the weir included angles that were tested.

Emiroglu *et al.* (in press) gave the Eq. (3) for the triangular labyrinth side weirs. This equation was developed for $(h_1-p) \geq 30$ mm. In which, (h_1-p) is nap height (i.e., water head above the weir). Moreover, Eq. (3) is valid for $45° \leq \theta \leq 150°$ in subcritical flow regime.

$$C_d = 0.4 + \left[\begin{array}{l} -2.62 + 0.634\left(\dfrac{L}{B}\right)^{0.254} + 3.214\left(\dfrac{L}{\ell}\right)^{-0.122} - \\[2mm] -0.684\left(\dfrac{p}{h_1}\right)^{-0.4} + 0.122\left(\sin\left(\dfrac{\theta}{4}\right)\right)^{1.982} + 0.22 F_1^{2.458} \end{array} \right]^{3.857} \tag{3}$$

where the weir width L, the channel width B, the weir crest length ℓ, the height of weir crest p are in meters, the labyrinth side weir included angle θ is in degrees and Froude number F_1 is dimensionless. Determination coefficient of this equation (R^2) is 0.94. It should be noted that Eq. (3) is valid for labyrinth side weir with one cycle.
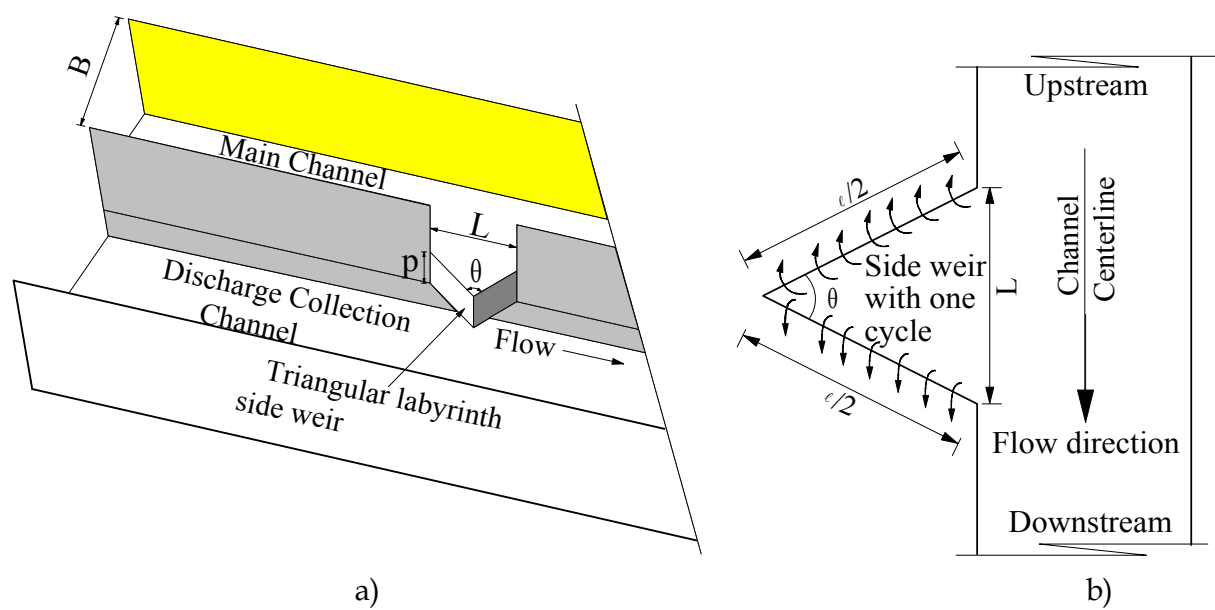

Fig. 3. Triangular labyrinth side weir: (a) Schematic view, (b) Plan view.

Fig. 4 shows the variation of Q_w/Q versus F_1 for constant crest height (p=0.20 m) and weir included angle (θ=45°). In which, Q_w is total flow over the side weir and Q is the discharge in the main channel before beginning of side weir. The ratio of Q_w/Q decreases with increasing Froude number. The primary reason is that the increase in the Q_w is less that that of Q. For example; Q_w is 14.62 L/s for Q=125 L/s, F_1=0.765, θ=45°, p=20 cm and L=50 cm.

Figure 5 shows that C_d is plotted against F_1. Obtained values for triangular labyrinth side-weirs having θ=45° for L/B=1.5 located on a straight channel were compared with the classical rectangular side-weir values. It is observed from Figure 5 that discharge coefficients of labyrinth side weirs have much higher values than those of rectangular side weirs. The crest length of labyrinth side-weir is always longer than that of classical rectangular side-weir. The main reason of labyrinth side-weir is to occur higher length of the crest and more severe secondary flow.
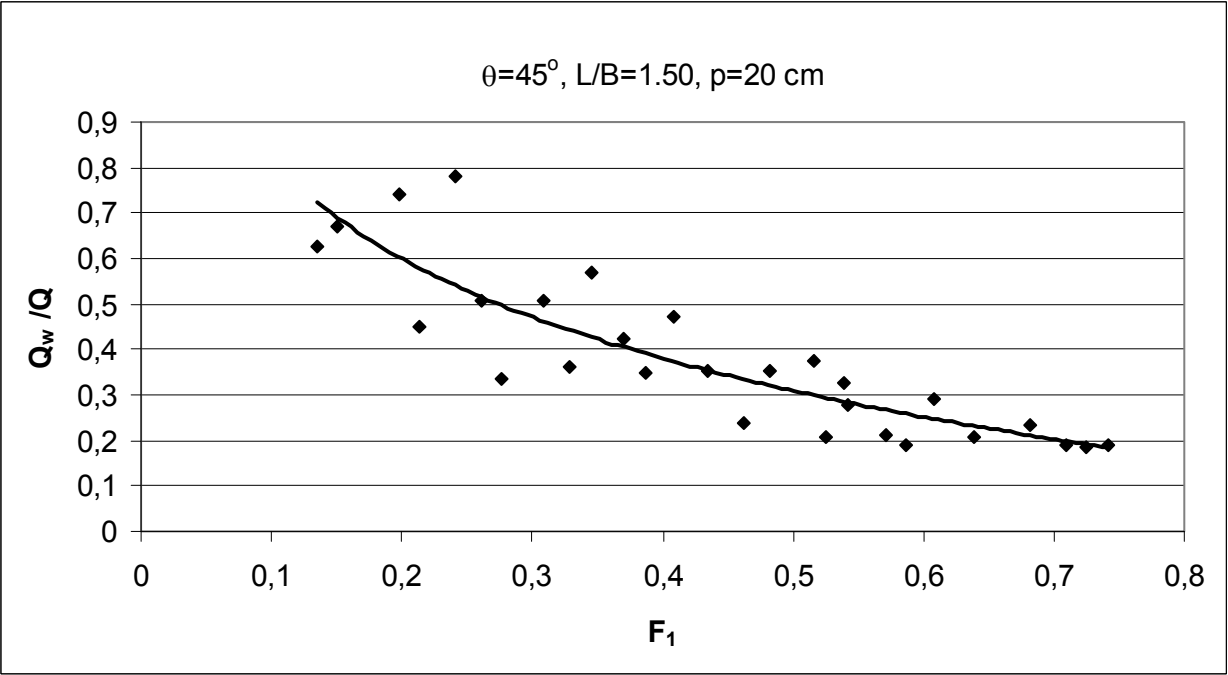
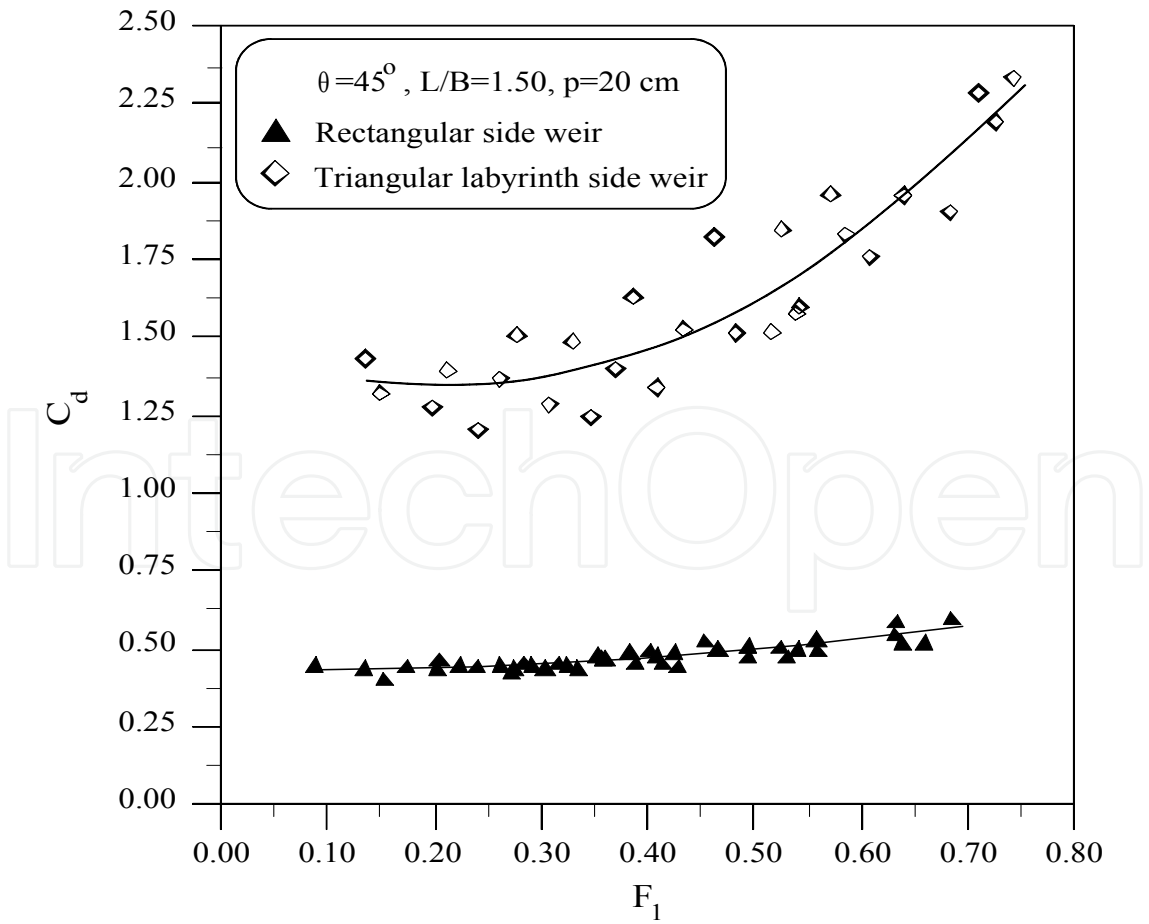Fig. 4. Variation of Q_w/Q versus F_1 for $\theta=45°$.

Fig. 5. Variations of C_d versus F_1

As it can be seen in Fig. 6 that as h_1-p/p ratio increases C_d values decrease. This situation is well known by hydraulic engineers. Tullis *et al.* (1995) and Falvey (2003) also stated that as nap height increase, discharge coefficient values decrease. Therefore, the designers should consider this important situation. It should be noted that the decreasing tendency in the discharge coefficient for the low weir included angles is higher than that of high weir included angles.
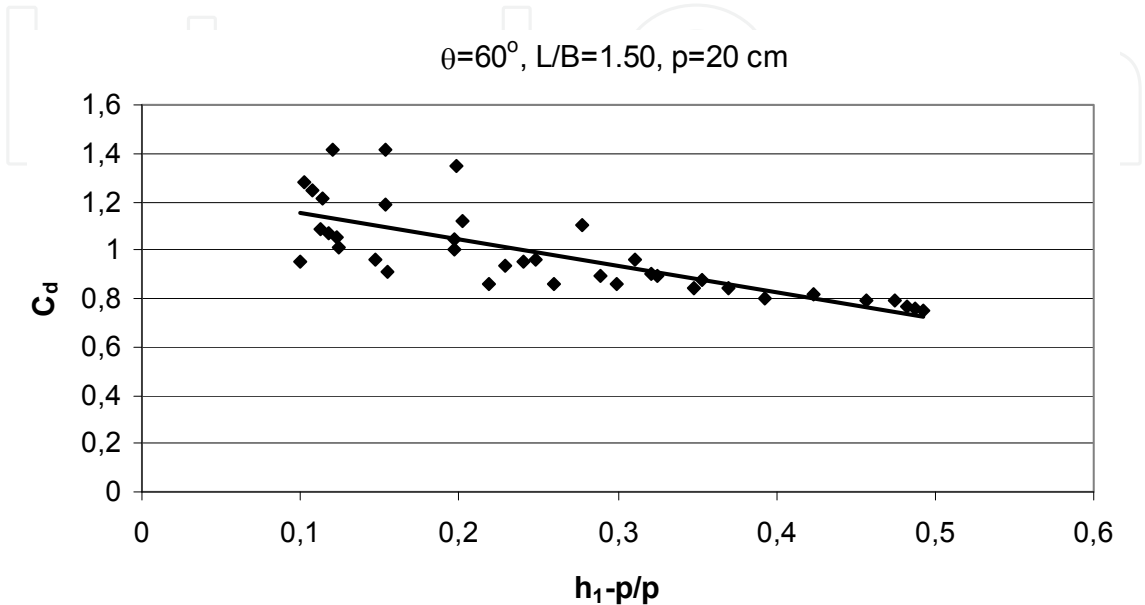

Fig. 6. Variation of C_d versus h_1-p/p for θ=60°

3.2 Trapezoidal labyrinth side weir

Figure 7 show schematic and plan view of a trapezoidal labyrinth side weir with one cycle. Laboratory experiments were carried out by Emiroglu & Kaya (2011) using a trapezoidal labyrinth side weir located on a straight channel. They obtained the following results regarding the labyrinth side weir discharge coefficient: (1) The discharge coefficients of trapezoidal labyrinth side weirs have much higher values than those of rectangular side weirs, but slightly higher than that of a triangular labyrinth side weir. The discharge coefficient C_d increases with reduction in sidewall angle. The primary reason for this may be the increased crest length. The intensity of secondary motion created by lateral flow increases with increasing overflow length. (2) The discharge coefficient of the trapezoidal labyrinth side weir is 1.5 to 5.0 times higher than for a rectangular side weir. (3) The values of the discharge coefficient C_d increase with an increase in p/h_1 and F_1 values. Moreover, the discharge coefficient C_d increases with increasing L/B ratio.

A nonlinear equation has been developed for the discharge coefficient of the trapezoidal labyrinth side weir. Minimum nap height at this equation is 30 mm.

$$C_d = \frac{\left[0.27 + 0.89F_1^{6.28} + 0.95\left(\dfrac{L}{B}\right)^{0.21}\right]^{2.42}}{\left[0.09 + 0.16\left(\dfrac{L}{\ell}\right)^{-1.66} - 6.86\left(\dfrac{p}{h_1}\right)^{0.75} + 14.22\left(\sin\alpha\right)^{0.62}\right]^{0.60}} \tag{4}$$

where Froude number $F_1(=V_1/(g.h_1)^{1/2})$ is dimensionless, the discharge coefficient C_d is dimensionless, the crest height of the side weir p, the width of the side weir $L(=2(2c+d.\sin\alpha))$, the width of the main channel B, the overflow length of the side weir ℓ (=2d+4c), the depth of flow at the upstream end of the side weir in the main channel centerline h_1 are in meters, and the sidewall angle α is degrees.
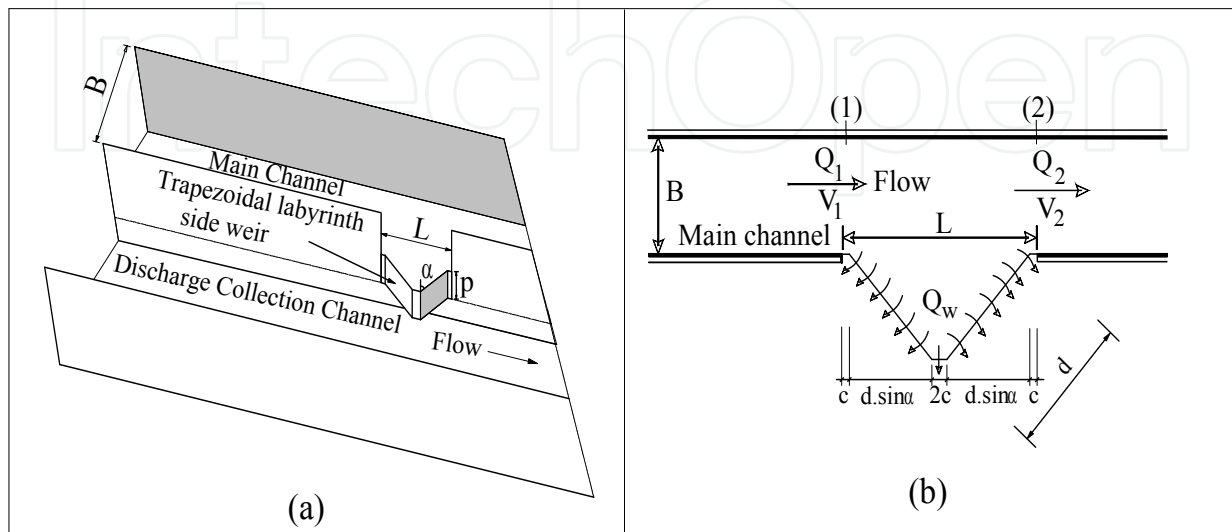

Fig. 7. Trapezoidal labyrinth side weir: (a) Schematic view, (b) Plan view

Equation 4 is valid for $16° \leq \alpha \leq 30°$. Correlation coefficient (R) of Eq. (4) is 0.97. It should be noted that the discharge coefficient of the trapezoidal labyrinth side weir is calculated for a single (i.e. a control section) cycle. The C_d that is calculated is substituted into Eq. (1). The depth of flow (h) in Eq. (1) is taken as the flow depth at upstream end of side weir at channel center (h_1).

Fig. 8 shows the variation of Q_w/Q versus F_1 for the crest heights (p=0.12, 0.16 and 0.20 m) and weir included angle (θ=45°). As mentioned above, the ratio of Q_w/Q generally decreases with increasing Froude number.

The values of C_d were plotted against F_1, as shown in Fig. 9. The values obtained for trapezoidal labyrinth side weirs having sidewall angle of α=30°, L/B=1.5 and the ratio of weir crest height to upstream flow depth [p/B=0.24, 0.32 and, 0.40] located on a straight channel were compared with values for the classic rectangular side weir. The discharge coefficients of trapezoidal labyrinth side weirs were found to have much higher values than those of rectangular side weirs. In other words, the discharge over trapezoidal labyrinth side weirs is greater than that over an equivalent straight weir. The overflow length of the trapezoidal labyrinth side weir is always longer than that of a classic rectangular side weir. The main reason is the greater length of the crest and the more severe secondary flow in trapezoidal labyrinth side weirs.

As h_1-p/p ratio increases C_d values decrease, as illustrated in Fig. 10. As mentioned above, this situation is very important for low sidewall angles because decreasing tendency in discharge coefficient for low sidewall angles is higher than that of high sidewall angles. This situation should be considered in the hydraulic design. To reduce the nap height, the labyrinth side weir can be selected as multi-cycles (see Fig. 11).
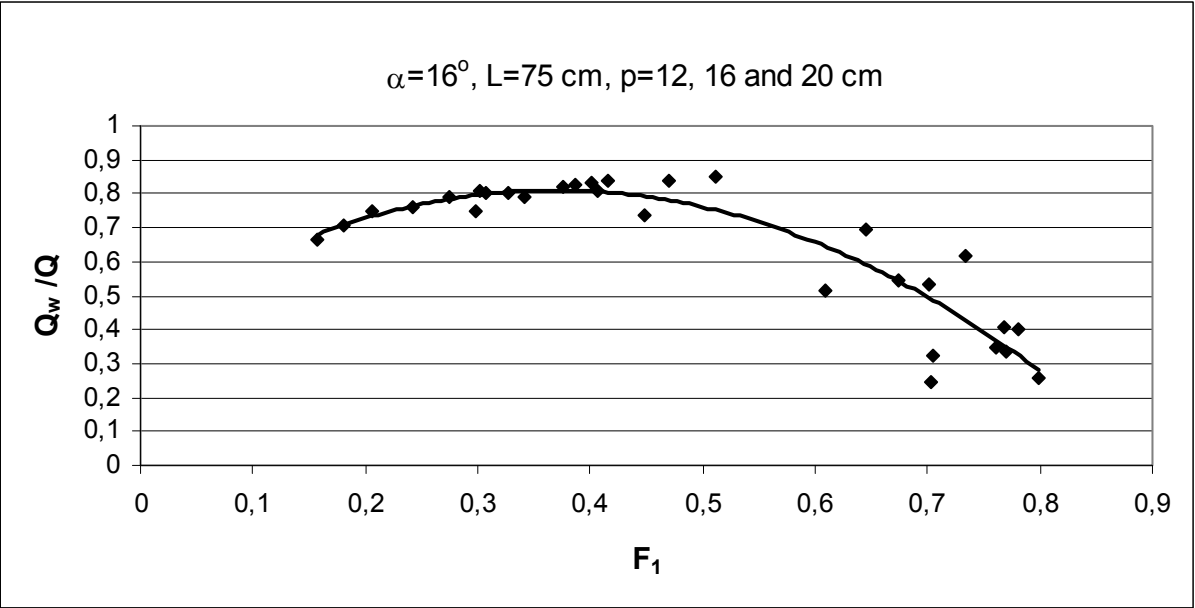
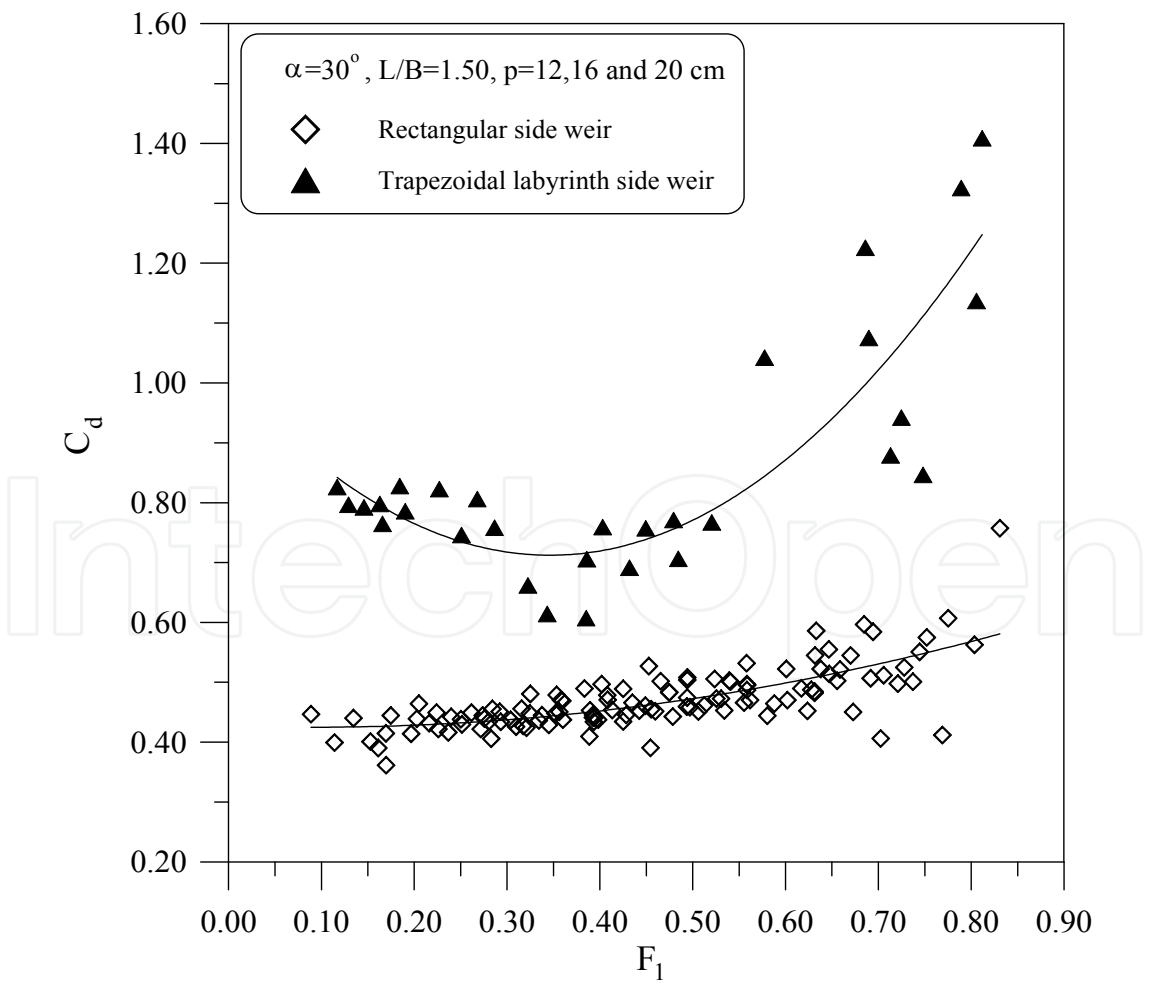Fig. 8. Variation of Q_w/Q versus F_1 for $\alpha=16°$.

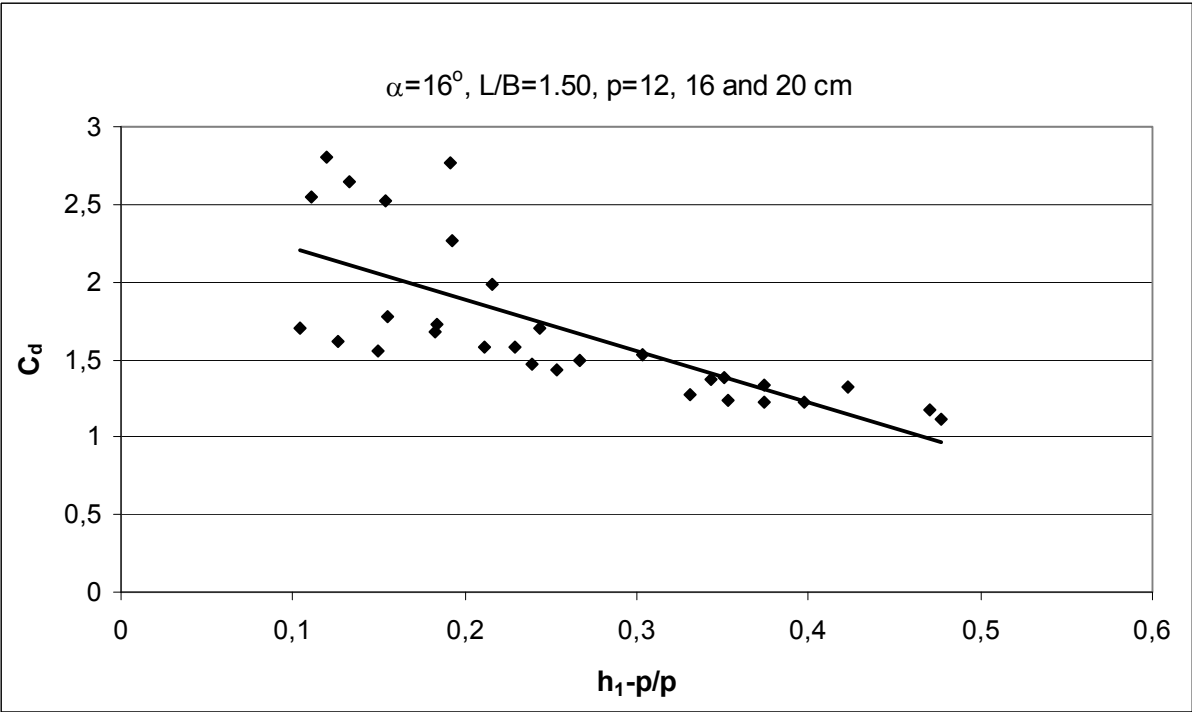Fig. 9. Variations of C_d versus F_1.

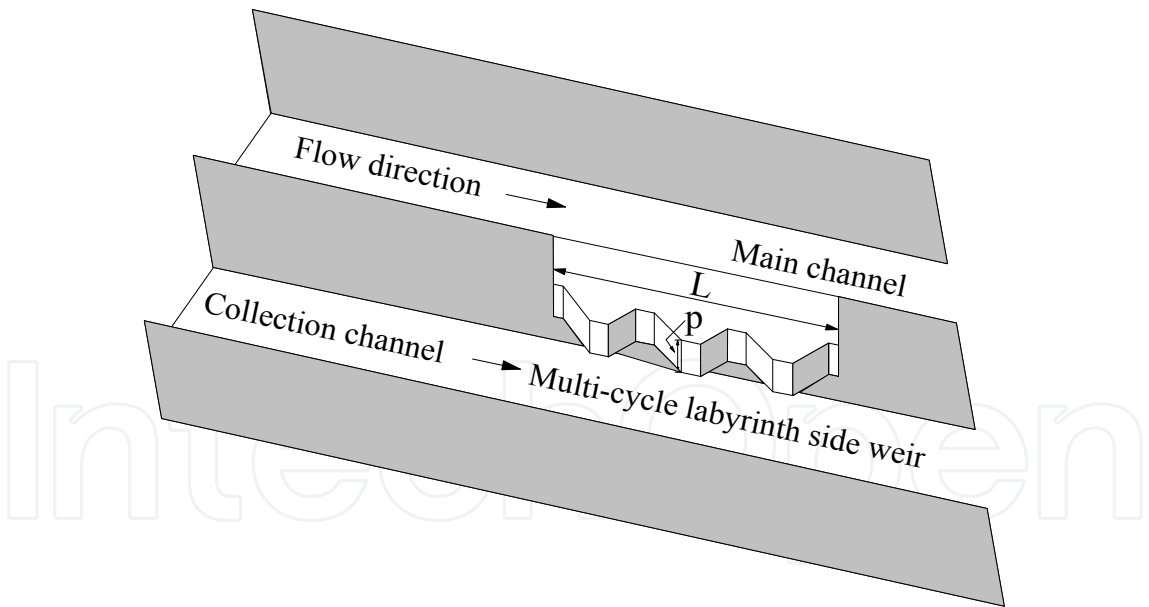Fig. 10. Variation of C_d versus h_1-p/p for α=16°.

Fig. 11. Trapezoidal labyrinth side weir with multi-cycle.

3.3 Semi-elliptical labyrinth side weir

Figure 12 show schematic and plan view of a semi-elliptical labyrinth side weir with one cycle. Laboratory experiments using a semi-elliptical side weir located on a straight channel were carried out, in order to investigate the effect of the dimensionless parameters F_1, p/h_1, L/B, L/ℓ and b/a on the discharge coefficient (Kaya *et al.*, 2011). They obtained the following

results regarding the labyrinth side weir discharge coefficient: (1) As a result of dimensional analysis, the following dimensionless parameters were found; $C_d = f(F_1, L/B, L/\ell, p/h_1, b/a)$. (2) The discharge coefficient of the semi-elliptical side weir is higher than that of the rectangular side weir, but lower than that of the triangular and trapezoidal labyrinth side weirs. (3) The discharge coefficient C_d increases with increasing L/B ratio.

Fig. 12. Semi-elliptical side weir: (a) Plan view, (b) Longitudinal section.

An ellipse is the finite or bounded case of a conic section, the geometric shape that results from cutting a circular conical or cylindrical surface with an oblique plane. It is also the locus of all points of the plane whose distances to two fixed points add to the same constant. By using an appropriate coordinate system, the ellipse can be described by the canonical implicit equation

$$\frac{x^2}{a^2} + \frac{y^2}{b^2} = 1 \tag{5}$$

where, (x,y) are the point coordinates in the canonical system. In this system, the center is the origin $(0,0)$ and the foci are $(-ea,0)$ and $(+ea,0)$. a is called the *major radius*, and b is the *minor radius*. The quantity $e = \sqrt{(1 - b^2/a^2)}$ is the *eccentricity* of the ellipse (Fig. 13).

Fig. 13. The ellipse and some of its mathematical properties.

A nonlinear equation has been developed for the discharge coefficient of the semi-elliptical side weir. Minimum nap height was taken as 30 mm when Eq. (6) was developed.

$$C_d = \frac{\left[-0.025\,\mathrm{F_1}^{0.10} + 0.16\left(\dfrac{L}{B}\right)^{2.72}\right]^{0.05}}{\left[53.15\left(\dfrac{L}{\ell}\right)^{0.61} - 9.71\left(\dfrac{p}{h_1}\right)^{0.12} - 22.07\left(\dfrac{b}{a}\right)^{0.18}\right]^{0.17}} \qquad (6)$$

where Froude number $\mathrm{F_1}$ is dimensionless, the discharge coefficient C_d is dimensionless, the crest height of the side weir p, the width (length) of the side weir L, the width of the main channel B, the major radius of ellipse a, the minor radius of ellipse b, the overflow length of side weir ℓ, and the depth of flow at the upstream end of the side weir in the main channel centerline h_1 are in meters.

Equation 6 is valid for $0.50 \le b/a \le 1.50$. It should be noted that the discharge coefficient of the semi-elliptical side weir is calculated for a single cycle. Correlation coefficient (R) of Eq. (6) is 0.93.

Figure 14 shows the variation of Q_w/Q versus $\mathrm{F_1}$ for the crest heights (p=0.12, 0.16 and 0.20 m) and b/a=0.50. As mentioned above, the ratio of Q_w/Q generally decreases with increasing Froude number. This situation is similar to the other labyrinth side weirs.
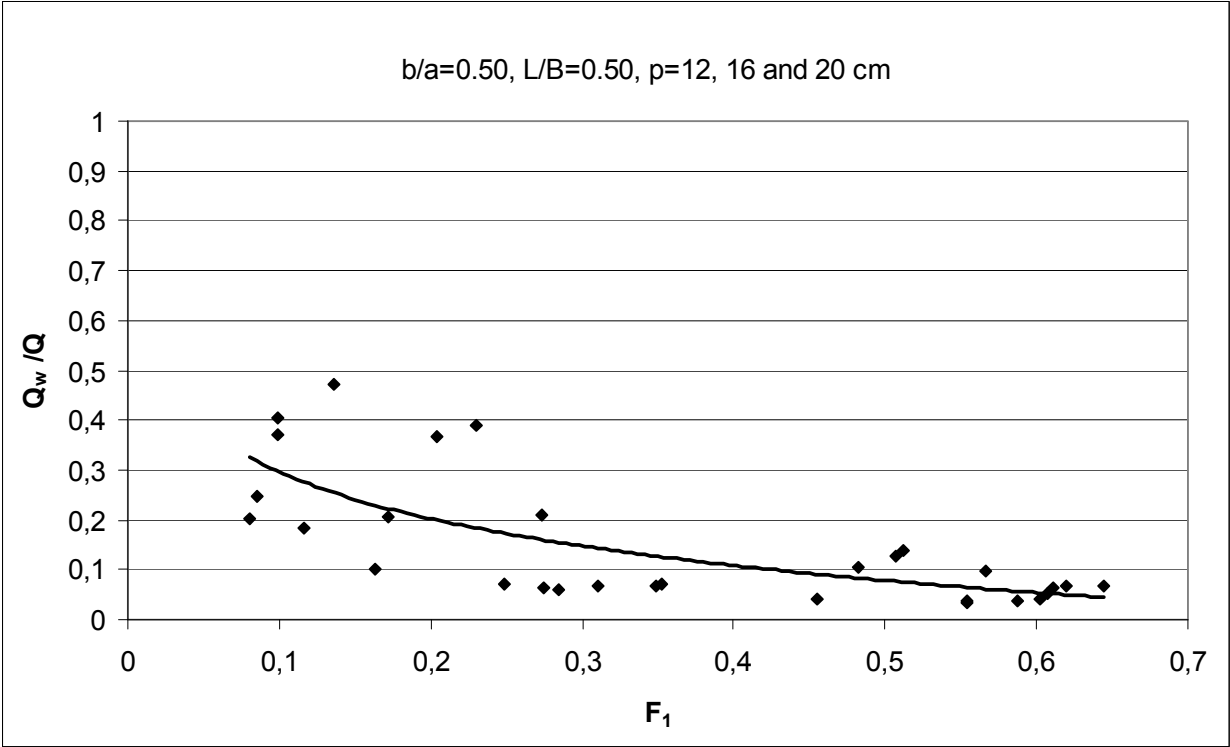
Fig. 14. Variation of Q_w/Q versus $\mathrm{F_1}$ for b/a=0.50.

C_d is plotted against $\mathrm{F_1}$, together with the values of the discharge coefficient of the rectangular side weir for the dimensionless ellipse radius b/a=1.50 and the dimensionless weir length L/B=1.50, as shown in Fig. 15. Figure 15 was plotted for p=12, 16 and 20 cm. The discharge coefficients of semi-elliptical side weirs have much higher values than those of rectangular side weirs. In other words, the discharge over semi-elliptical labyrinth side

weirs is greater than that over an equivalent straight weir in the ratio of the weir sill lengths. In particular, the semi-elliptical side weir with b/a=1.50 has higher C_d values. The overflow length of the semi-elliptical side weir is always longer than that of a classical rectangular side weir. The main reason is the higher length of the crest and the more severe secondary flow in semi-elliptical side weirs.
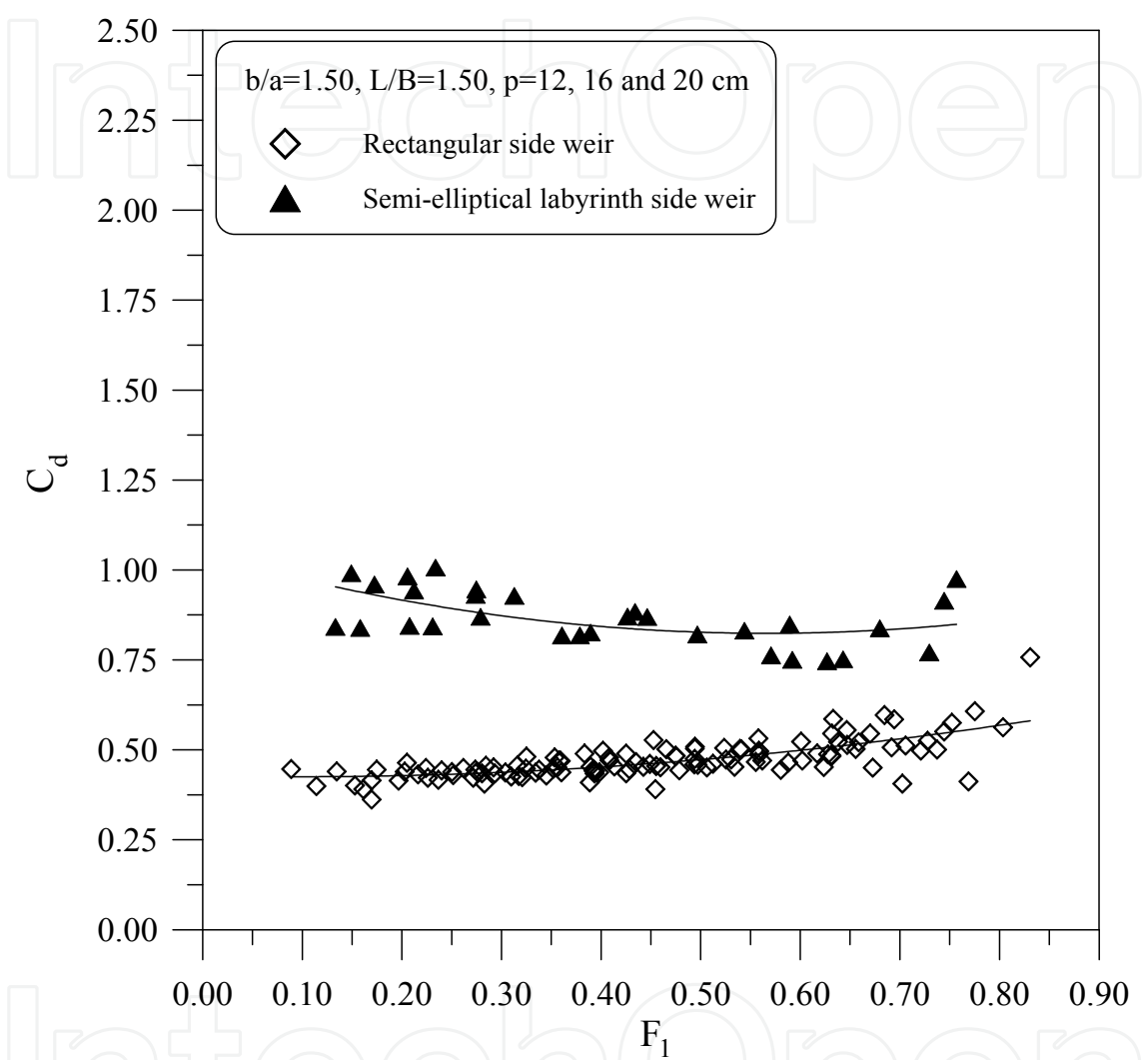

Fig. 15. Variations of C_d versus F_1.

Figure 16 shows the variation of C_d versus h_1-p/p ratio. The values of C_d decrease as h_1-p/p increases. It should be noted that decreasing tendency in Cd values is lower than that of triangular and trapezoidal labyrinth side weirs. This side weir also can be used as multi-cycles. Thus, the total crest length increases and the nap height over the weir decreases for a constant main channel discharge.

Consequently, to select trapezoidal labyrinth weir is more appropriate due to some reasons: For example, (1) Discharge coefficient of the trapezoidal labyrinth side weir is higher than that of the other labyrinth side weir types. (2) Its construction is easy in accordance with the other types. (3) The classical labyrinth weirs are also constructed as trapezoidal-shaped.

It should be noted that labyrinth side weirs can be constructed as multi-cycles (see Fig. 17). In this case, nap height decreases, discharge capacity over the weir increases.
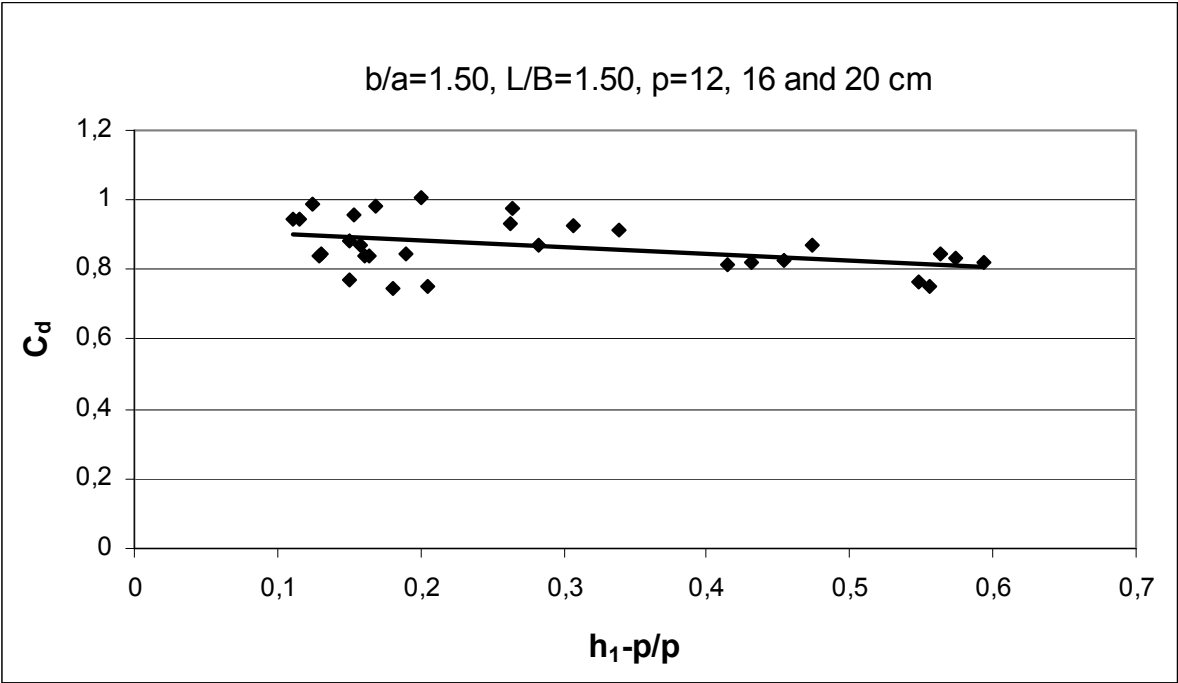
Fig. 16. Variation of C_d versus $h_1\text{-}p/p$ for α=16°.

(a) Trapezoidal labyrinth side weir

(b) Triangular labyrinth side weir

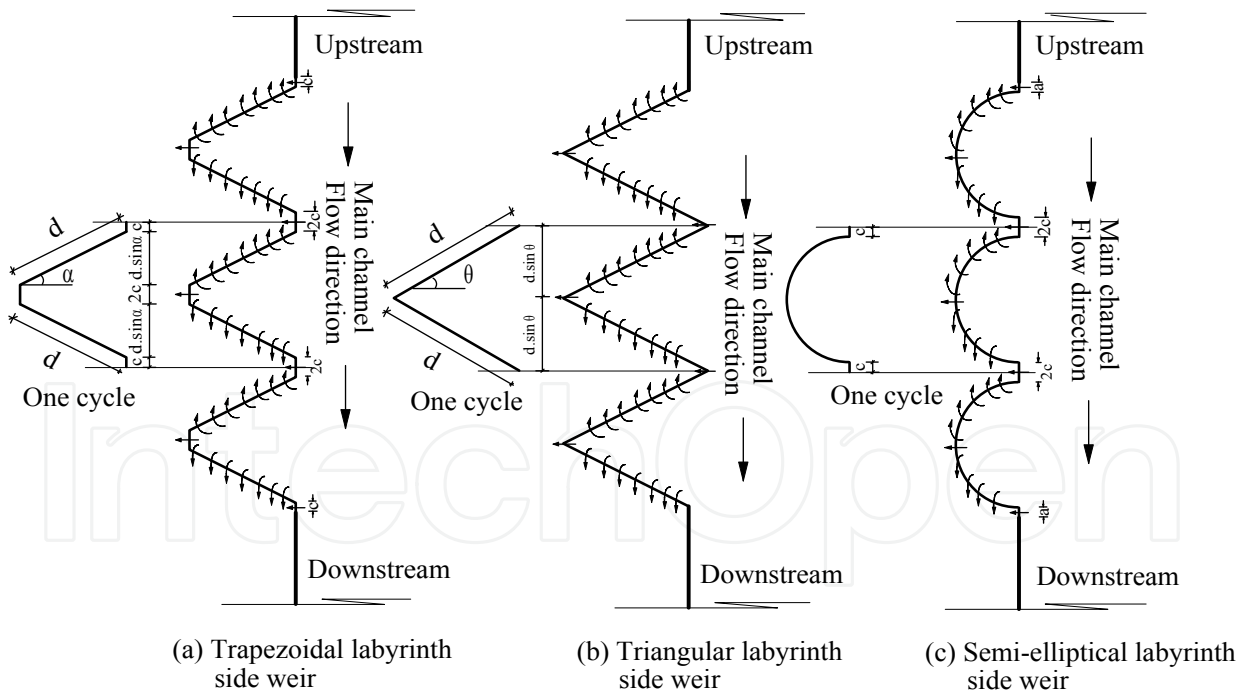(c) Semi-elliptical labyrinth side weir

Fig. 17. Plan views of the labyrinth side weirs with multi-cycles.

4. Clear-water scour at labyrinth side weir intersection along the bend

Scour around hydraulic structures (for example; grade-control structures, pipe outlets, stilling basins, obstacles, bridge piers and lateral intakes) is a natural phenomenon by the

flow of water in rivers and streams. Around these hydraulic structures, scouring introduces the possibilities of a reduction in the support given to foundations of these structures. Depths of scour can be seen to depend on the properties of the bend material in the stream (particle shape and size, grading, layering, alluvial or cohesive), the foundation geometries and the properties of flow (Raudkivi, 1986; Agaccioglu & Onen, 2005). Melville & Chiew (1999) reported that clear-water scour occurs for mean flow velocities, V, up to the threshold velocity for bed sediment entrainment, V_c, that is while live bed scour occurs for $V>V_c$. At the clear-water flow conditions, the local depth of scour in a uniform sediment increases almost linearly with flow intensity to a maximum value at the threshold velocity ($V=V_c$) (Agaccioglu & Onen, 2005).

A number of experiments for investigating the development of a scour hole geometry around a triangular labyrinth side weir are carried out with a model located on a rectangular plexiglas flume at the Hydraulic Laboratory of Firat University, Elazig, Turkey. The main and collection channels were located between two straight channels at a central angle of 180° with 3.00 and 3.50 m radius to the centerline, respectively. The bend is connected with an upstream straight reach of 13.30 m and a downstream straight reach of 3.00 m. The main channel is 0.50 m wide and 0.60 m deep with a well-painted bottom. The collection channel is 0.75 m deep, 0.50 m wide and situated parallel to the main channel. Details of the channel are shown in Fig. 2. Uniform bed materials are placed as a 20 cm thick layer in the main channel with a bed slope of 0.001. The bed material of the main channel was well mixed to prevent sediment grading and layering, and then flattened before each run. During the experiments, the upstream valve is adjusted slowly without causing any disturbance to the bed material until the desired flow conditions are obtained in the flume. No sediment inflow is allowed from upstream due to clear-water conditions. Triangular labyrinth side weirs were first placed at the 30° section of the bend centre and then at the 150° section of bend centre. Three different weir crest heights (0.07, 0.12 and 0.17 m) of the triangular labyrinth side weir were taken in this study.

The water depth was controlled by a sluice gate located at the end of the main channel to produce the uniform flow. Water was supplied from an overhead tank with a constant head and measured by an electromagnetic flowmeter (Siemens brand name). Moreover, the flow rate was also calibrated 90° V-notched weir (Q_1) at the beginning of the main channel. Side weir discharge at the end of the downstream of the collection channel (Q_w) was measured by calibrated a 90° V-notched weir. Thus, the downstream discharge (Q_2) in the main channel is obtained as:

$$Q_2 = Q_1 - Q_w \tag{7}$$

The measurements of water surfaces and bed levels are determined using digital point gauge with a capability of reading to the nearest 0.01 mm. In the present study, the mean particle size of the bed material (d_{50}) is 1.16 mm. The critical velocity (V_c) of motion of initiation is determined using a Shields diagram with a series of test runs which led to the following formula:

$$V_c = 0.1557.\log(4767.h_1) \tag{8}$$

where the flow depth at the upstream end of triangular labyrinth side weir at the channel centre h_1 is in meters and the critical velocity at the threshold conditions or initiation of motion V_c is in m.s^{-1}.

Figure 18 shows the development of clear-water scour with time in a curved channel when α=30°, θ=90°, L/B=0.50 and p/B=0.14. In other words; chute angle, weir included angle, dimensionless weir length and dimensionless crest height are constant in this figure, but approach flow intensity, V_1/V_c, is variable. Here, the weir opening length, L, is 25 cm, total crest length of the labyrinth side weir is 35.36 cm. Moreover, the crest height is 7 cm. As shown in Fig. (17), as V_1/V_c increases the depth of scour at the side-weir intersection, H, also increases. At the first 200 minutes, the increasing tendency in the scour depth is high. That is, the scour depth increases rapidly with time at the beginning. The increasing tendency in the scour depth is quietly low after from 600 minutes. Finally, the depth of clear-water scour approaches the equilibrium depth of scour, H_d, asymptotically with time, depending on flow intensity. In addition, there is no scour for approach flow intensities less than V_1/V_c=0.50 in the experimental study.
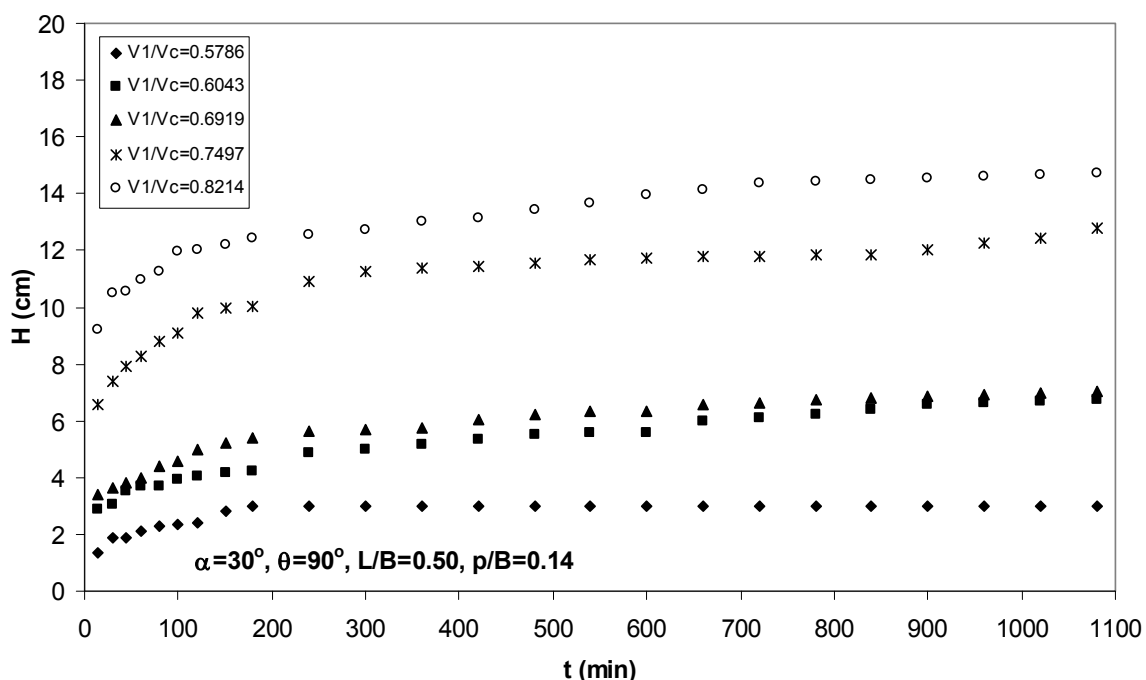
Fig. 18. The development of clear-water scour with time in a curved channel when α=30°, p=7 cm and θ=90°.

Figure 19 shows that the depth of scour at the side-weir intersection, H, is plotted against the temporal time, t, for α=150°. The increasing tendency of scour hole at the first 200 minutes for α=150° is higher than that of α=30°. Emiroglu *et al.* (2010) stated that the discharge capacity at the α=150° has the highest values according to the other angle of bend center (i.e., α=30, 60, 90 and 120°). Therefore, the intensity of the secondary motion is high at the angle of the bend center of 150°. Thus, higher scour holes generally were obtained at the angle of bend center of 150.

As is well known, the water intake structures in a curved river are generally located at the last part of the bend. Therefore, experiments are also conducted to determine the development of the depth of scour at the 150° section of the bend centre in order to understand the effect of time to scour depth for clear water. Figure 20 and Fig. 21 show the development of clear-water scour versus time. As shown in Figs. 20 and 21, the depth of
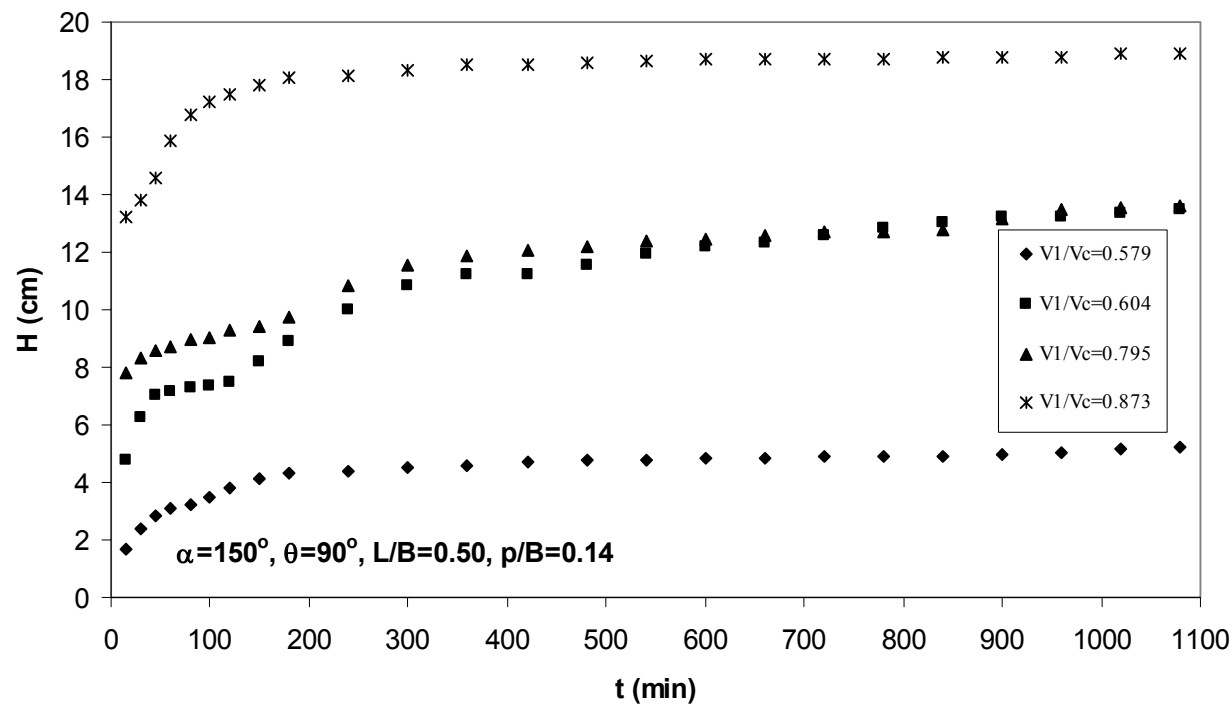
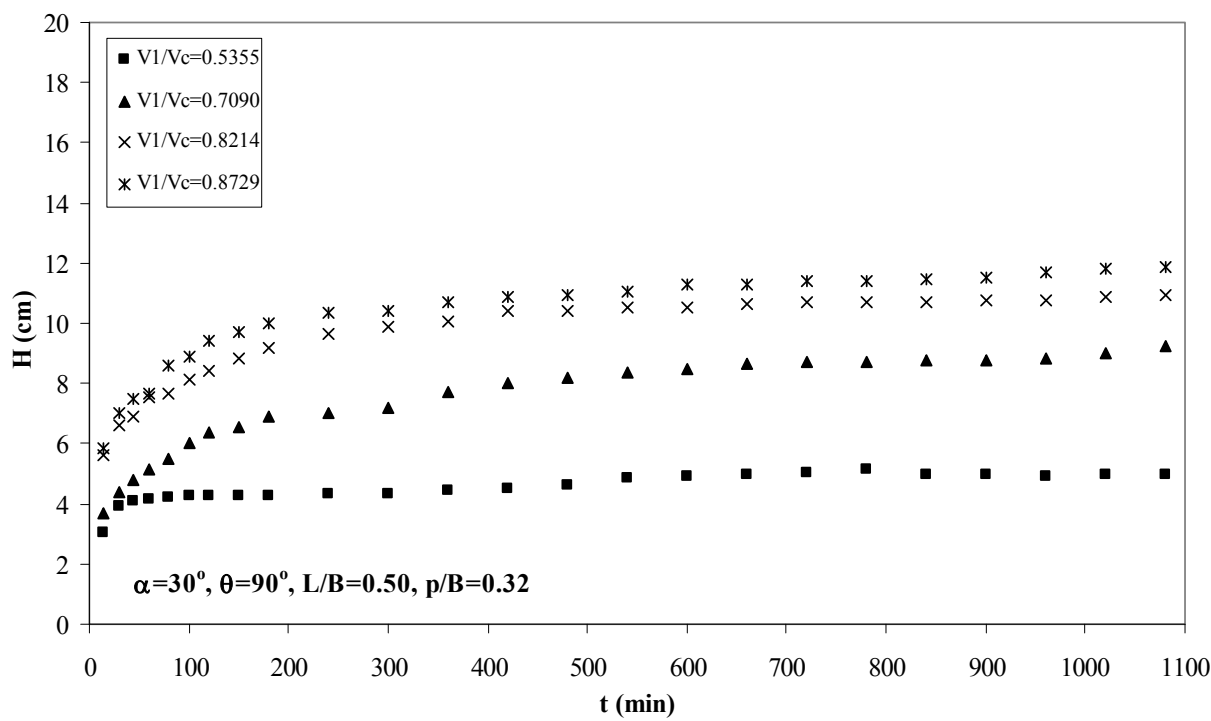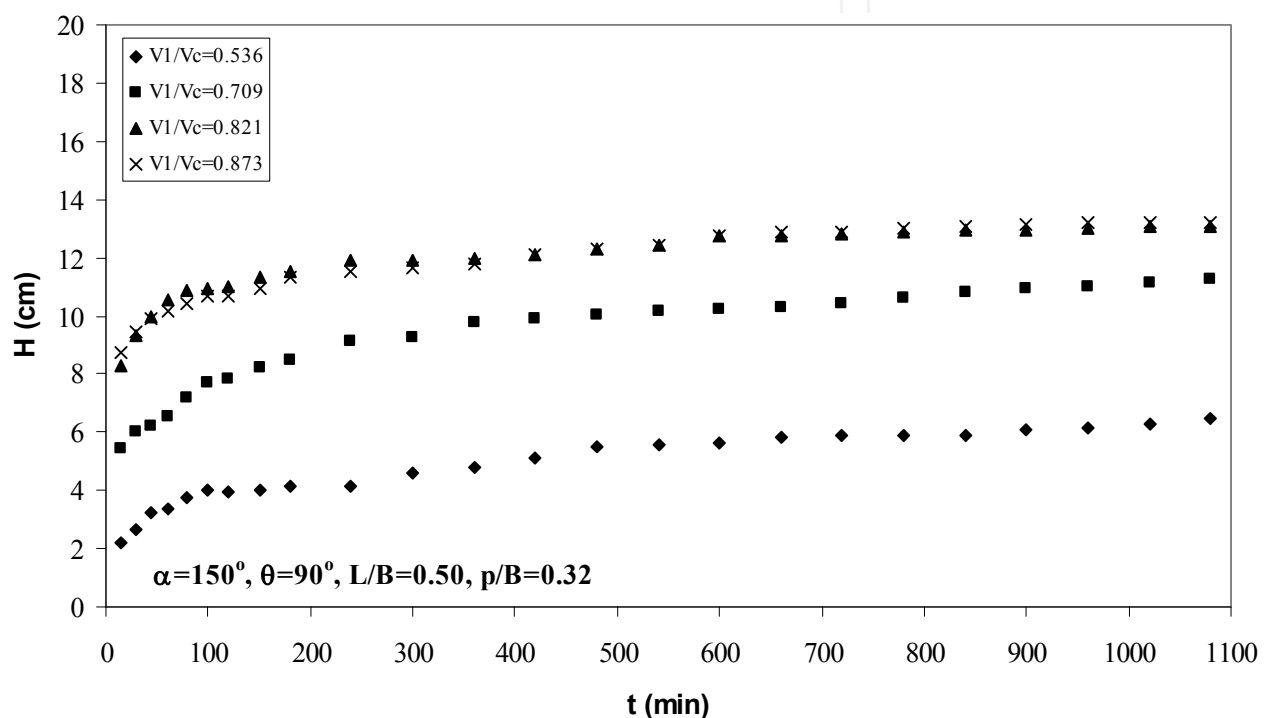Fig. 19. The development of clear-water scour with time in a curved channel when α=150°, p=7 cm and θ=90°.

Fig. 20. The development of clear-water scour with time in a curved channel when α=30°, p=16 cm and θ=90°.

scour increases rapidly with time at the beginning, and then asymptotically approaches stable values. That means that the scour depth reaches an equilibrium condition. Time to equilibrium depends on the approach flow intensity and the dimensionless side weir crest height. When the flow intensity increases, time to the equilibrium depth of scour increases. As mentioned before, the intensity of the secondary circulation caused by the lateral flow increases with an increase of the overflow length because of the remaining momentum in the main channel. This also causes much scour around the side-weir intersection.

Fig. 21. The development of clear-water scour with time in a curved channel when α=150°, p=16 cm and θ=90°.

Figure 22 shows bed topography at a side weir intersection when V/V_c=0.7090, α=30°, θ=90°, L/B=0.50 and p/B=0.32. Figure 22 shows bed topography at a side-weir intersection when α=30°, θ=90°, V/V_c=0.8214, L/B=0.50 and p/B=0.32. As seen from Figures 22 and 23, maximum scour hole approximately occurs either at end the downstream of the triangular labyrinth side weir, or after from the end of the downstream of the triangular labyrinth side weir. V_1/V_c is a significant parameter for scour hole geometry and location of the maximum scour hole. As mentioned above, as V_1/V_c increase H also increase. At the downstream end of the triangular labyrinth side weir, a longitudinal bar in the middle of the channel and scour hole close the outer bank are formed because of the changes in shear stress field and velocities (see Fig. 22).
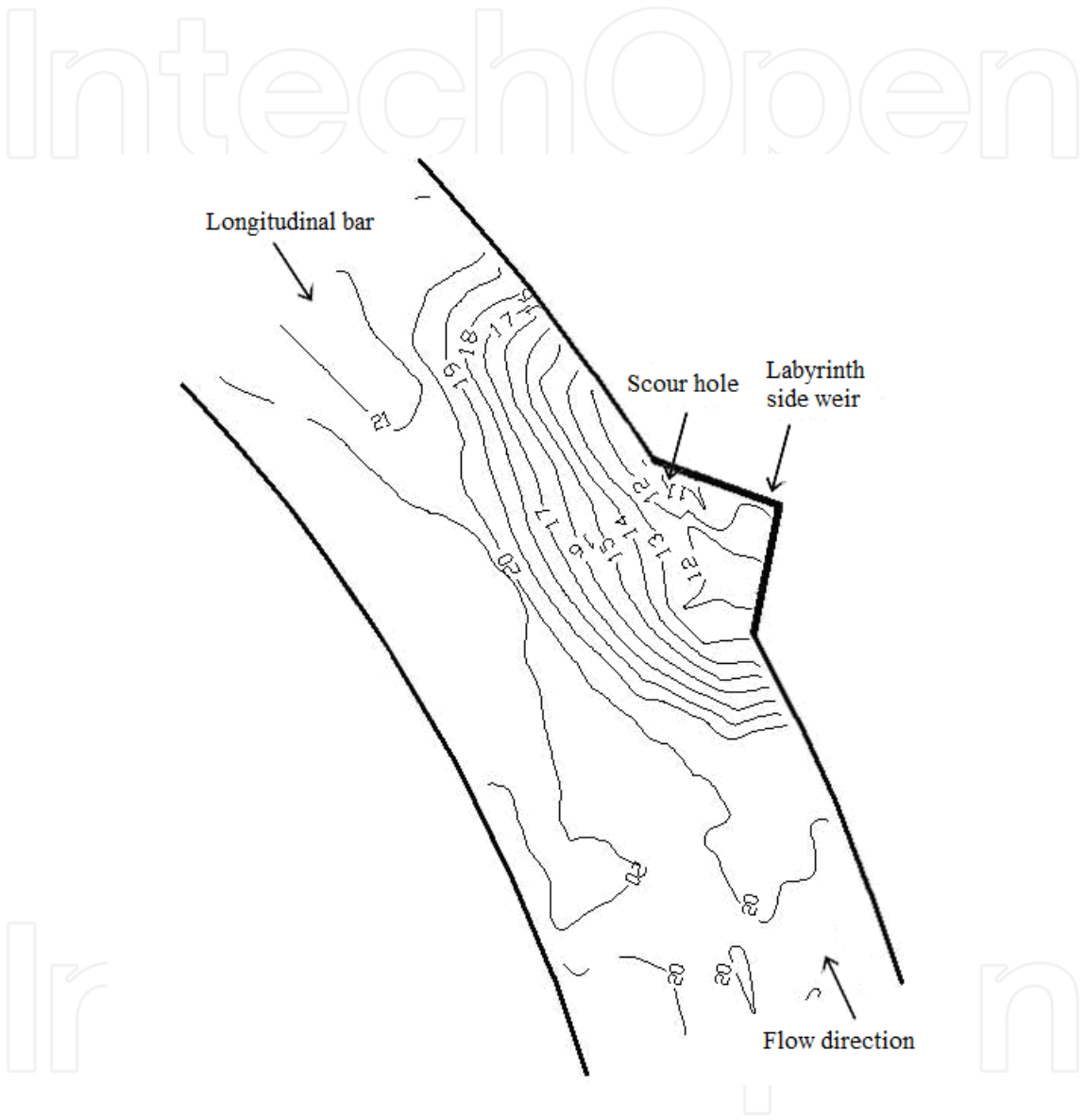
Fig. 22. Bed topography at a side weir intersection when V/V_c=0.7090, α=30°, θ=90°, L/B=0.50 and p/B=0.32 (*contours in cm and undisturbed bed level is 20 cm*).
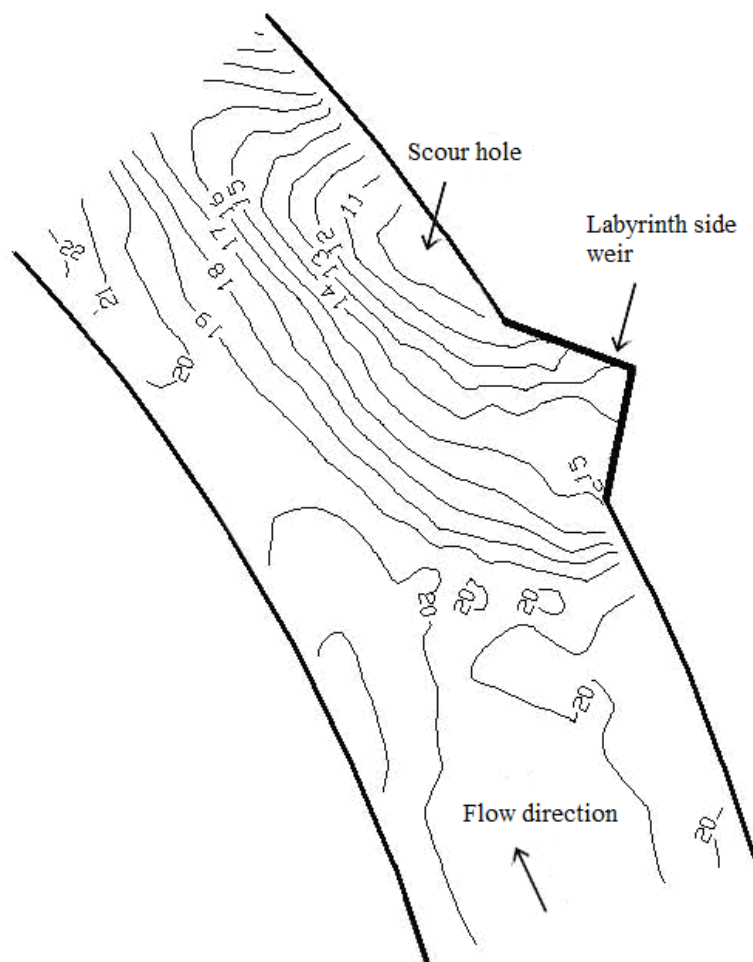
Fig. 23. Bed topography at a side weir intersection when α=30°, θ=90°, V/V_c=0.8214, L/B=0.50 and p/B=0.32 (*contours in cm and undisturbed bed level is 20 cm*).

5. Conclusions

Laboratory experiments, within the Tubitak Project (MAG 104M394), were carried out using triangular, trapezoidal and semi-elliptical labyrinth side weirs located on a straight and curved channel in order to investigate the discharge coefficient and the scour topography at the side-weir intersection area. Empirical correlations were submitted, predicting the discharge coefficient of these labyrinth side weirs. The following conclusions can be drawn from these findings:

- The discharge coefficients of labyrinth side weirs have much higher values than those of classical rectangular side weirs. The primary reason for this may be the increased crest length. The intensity of secondary motion created by lateral flow increases with increasing overflow length.
- The discharge coefficient of the labyrinth side weir is 1.5 to 5.0 times higher than for a rectangular side weir.
- The values of the discharge coefficient C_d increase with an increase in dimensionless crest height p/h_1 and Froude number F_1 values. Moreover, the discharge coefficient C_d increases with increasing dimensionless weir opening length L/B ratio.
- The flow intensity V_1/V_c is a significant parameter for scour hole geometry and location of the maximum scour hole.

- As the flow intensity V1/Vc increases the depth of scour at the side-weir intersection, H, also increases.
- The depth of scour increases rapidly with time at the beginning, and then asymptotically approaches stable values.
- Maximum scour hole approximately occurs either at end the downstream of the triangular labyrinth side weir or after from the end of the downstream of the triangular labyrinth side weir.
- At the downstream end of the triangular labyrinth side weir, a longitudinal bar in the middle of the channel and scour hole close the outer bank are formed because of the changes in shear stress field and velocities.

6. Acknowledgments

7. References

Agaccioglu H. & Onen F. (2005). Clear-water scour at a side-weir intersection along the bend. *Irrigation and Drainage*, Vol. 54, pp. 553-569.

Borghei M., Jalili M. R. & Ghodsian M. (1999). Discharge coefficient for sharp-crested side weir in subcritical flow. *J Hydraulic Eng ASCE*. Vol. 125, No. 10, pp. 1051-1056

De Marchi G. (1934). Saggio di teoria de funzionamente degli stramazzi letarali. *L'Energia Elettrica, Rome, Italy*, Vol. 11, No. 11, pp. 849-860

Emiroglu M. E., Kaya N. & Ozturk M. (2007). Investigation of Labyrinth Side Weir Flow and Scouring at the Lateral Intake Region in a Curved Channel. *The Scientific and Technological Research Council of Turkey (TUBITAK), Engineering Science Research Grant Group*, Project No: 104M394 [in Turkish]; 253p.

Emiroglu M.E., Kaya N. & Agaccioglu H. (2010). Discharge capacity of labyrinth side weir located on a straight channel. *J Irrig Drainage Eng ASCE*, Vol. 136, No. 1, pp. 37-46.

Emiroglu, M. E. & Kaya, N. (2011). Discharge coefficient for trapezoidal labyrinth side weir in subcritical flow. *Water Resources Management*, Vol. 25, pp. 1037-1058.

Emiroglu M. E., Kaya N. & Agaccioglu, H. Closure to "Discharge Capacity of Labyrinth Side-Weir Located on a Straight Channel. *J Irrig Drainage Eng ASCE*, in press.

Falvey H. T. (2003). Hydraulic design of labyrinth weirs. *American Society of Civil Engineers*, Virginia, 161p.

Kaya N., Emiroglu M. E. & Agaccioglu H. (2011). Discharge coefficient of semi-elliptical side weir in subcritical flow. *Flow Measurement and Instrumentation*, Vol. 22, pp. 25-32.

Melville B.W. & Chiew Y. M. (1999). Time scale for local scour at bridge scours. *Journal of Hydraulic Engineering ASCE*, Vol. 125, No. 1, pp. 59-65.

Novak P. & Cabelka J. (1981). Models in Hydraulic Engineering, *Pitman Publishing Limited*, London.

Raudkivi A. J. (1986). Functional trends of scour at bridge piers. *Journal of Hydraulic Engineering ASCE*, Vol. 112, No. 1, pp. 1-13.

Tullis J. P., Nosratollah A., Waldron D. (1995). Design of labyrinth spillways. *J Hydraulic Eng ASCE*, Vol. 121, No. 3, pp. 247-255.
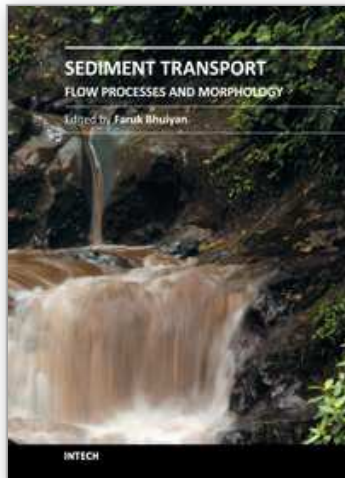
Sediment Transport - Flow and Morphological Processes

Edited by Prof. Faruk Bhuiyan

The purpose of this book is to put together recent developments on sediment transport and morphological processes. There are twelve chapters in this book contributed by different authors who are currently involved in relevant research. First three chapters provide information on basic and advanced flow mechanisms including turbulence and movement of particles in water. Examples of computational procedures for sediment transport and morphological changes are given in the next five chapters. These include empirical predictions and numerical computations. Chapters nine and ten present some insights on environmental concerns with sediment transport. Last two contributions deal with two large-scale case studies related to changes in the transport and provenance of glacial marine sediments, and processes involving land slides.

How to reference

In order to correctly reference this scholarly work, feel free to copy and paste the following:

M. Emin Emiroglu (2011). Clear-Water Scour at Labyrinth Side Weir Intersection Along the Bend, Sediment Transport - Flow and Morphological Processes, Prof. Faruk Bhuiyan (Ed.), ISBN: 978-953-307-374-3, InTech, Available from: http://www.intechopen.com/books/sediment-transport-flow-and-morphological-processes/clear-water-scour-at-labyrinth-side-weir-intersection-along-the-bend

INTECH
open science | open minds